Universal scaling of specific heat in the $S = \frac{1}{2}$ quantum kagome antiferromagnet herbertsmithite

H. Murayama,[1,*] T. Tominaga,[1] T. Asaba,[1] A. de Oliveira Silva,[1] Y. Sato,[1,2] H. Suzuki,[1] Y. Ukai,[1] S. Suetsugu,[1] Y. Kasahara,[1] R. Okuma,[3] I. Kimchi,[4] and Y. Matsuda[1]

[1]*Department of Physics, Kyoto University, Kyoto 606-8502, Japan*
[2]*RIKEN Center for Emergent Matter Science, Wako, Saitama 351-0198, Japan*
[3]*Clarendon Laboratory, University of Oxford, Parks Road, Oxford OX1 3PU, United Kingdom*
[4]*School of Physics, Georgia Institute of Technology, Atlanta, Georgia 30332, USA*

(Received 10 June 2021; revised 14 October 2022; accepted 17 October 2022; published 3 November 2022; corrected 27 April 2023)

Despite tremendous investigations, a quantum spin liquid (QSL) state realized in a spin-1/2 kagome Heisenberg antiferromagnet remains largely elusive. In herbertsmithite $ZnCu_3(OH)_6Cl_2$, a quantum spin liquid candidate on the perfect kagome lattice, precisely characterizing the intrinsic physics of the kagome layers is extremely challenging due to the presence of interlayer Cu/Zn antisite disorder within its crystal structure. Here we measured the specific heat and thermal conductivity of single-crystal herbertsmithite in magnetic fields with high resolution. Strikingly, intrinsic magnetic specific heat contribution arising from the kagome layers exhibits excellent scaling collapse as a function of T/H (temperature/magnetic field). In addition, no residual linear term in the thermal conductivity $\kappa/T(T \to 0)$ is observed in zero and applied magnetic fields, indicating the absence of itinerant gapless excitations. These results capture a new essential feature of the QSL state of the kagome layers; localized orphan spins are induced by exchange bond randomness, surrounded by a nonitinerant QSL.

DOI: 10.1103/PhysRevB.106.174406

I. INTRODUCTION

A quantum spin liquid (QSL) is an exotic state of matter where quantum fluctuations obstruct the formation of long-range magnetic order even in the zero-temperature limit. In QSLs, spins are quantum mechanically entangled over long distances without showing simple symmetry breaking, and they can form fractionalized collective excitations. For spin systems in dimensions higher than one, it is generally believed that frustrating interactions are required to stabilize the QSL states. Among this class of materials, the spin-1/2 two-dimensional (2D) kagome Heisenberg antiferromagnet with strong geometrical frustration has attracted considerable interest, as such a system is supposed to exhibit a QSL ground state [1]. However, understanding the nature of the kagome lattice has proved to be one of the most vexing issues in the quantum spin systems. In fact, despite tremendous research efforts, the ground state of the QSL in the kagome system remains unknown [2–17].

Currently, the most promising candidates are a gapped spin liquid with a Z_2 topological order [5,9,10,16] and a gapless $U(1)$ Dirac spin liquid [2,6,12,15]. Among kagome quantum magnets, herbertsmithite $ZnCu_3(OH)_6Cl_2$ has been most extensively studied as a canonical candidate for bearing a QSL state [18,19]. The crystal consists of 2D perfect kagome planes nearly fully occupied with Cu^{2+} ions, and a kagome lattice of spin-1/2 nearest-neighbor Heisenberg antiferromagnetic interactions is realized. The crystal structure of herbertsmithite contains interlayer sites primarily occupied by nonmagnetic Zn^{2+} ($S = 0$) [Figs. 1(a) and 1(b)] [20,21]. Some interlayer Zn sites are replaced by Cu, which induces antisite disorder within its crystal structure [22]. In contrast to the other kagome candidates, herbertsmithite does not exhibit magnetic ordering down to the lowest measured temperatures, despite large exchange interaction ($J/k_B \approx 180$ K) in the kagome layers [23–25]. The inelastic neutron scattering (INS) measurements revealed that excitations are dominated by an unusual broad continuum, which has been considered a signature of the fractional spinon excitations in the QSL [26].

A key question is to understand the intrinsic physics of the kagome layers in herbertsmithite, particularly magnetic and thermodynamic properties. Despite intensive experimental investigations, however, precisely characterizing the low-energy excitations within the kagome layers is challenging. In fact, recent studies have invoked different aspects of this compound, i.e., the interlayer Cu/Zn antisite disorder has a significant impact on these properties [27–32]. Although nuclear magnetic resonance (NMR) [31–33] and INS experiments [30] have been performed by several groups, whether the spin excitations are gapped or gapless is still controversial. Furthermore, interpretation of the most fundamental thermodynamic quantities, such as specific heat [34–39] and magnetic susceptibility [25,40–43], remains largely elusive. It has been suggested that the intrinsic specific heat of kagome layers may be seriously masked by the contribution from the antisite disorder, which dominates the total specific heat. The magnetic susceptibility exhibits a diverging Curie-like tail, suggesting that some of the Cu spins act as weakly coupled impurities [25].

Recently, a new mechanism for unusual features in thermodynamic quantities of quantum spin systems has been

*Present address: RIKEN Center for Emergent Matter Science, Wako, Saitama 351-0198, Japan.

introduced [44,45]. For this scenario, orphan spins are induced by randomness or disorder and form random singlets. In some quantum spin systems, including valence bond solids and QSLs with sufficient disorder, it has been proposed that low-temperature specific heat $C(H, T)$ in temperature T and magnetic field H exhibits T/H collapse, showing universal scaling features. The universal scaling appears as a result of a broad distribution of antiferromagnetic exchange interactions, which is a driving force of the formation of such random singlets. It has been pointed out that this scaling relation may hold in herbertsmithite [45]. In this scenario, observed specific heat could arise from the kagome layers, in contrast to previous interpretations. However, it is premature to judge the validity of this scaling collapse because of the following reasons. First of all, extra contributions to specific heat, such as phonon term and contribution arising from interlayer Cu/Zn antisite disorder, are not excluded from the measured $C(T)$, and hence it must be checked whether the scaling law is valid or not after subtracting these contributions. Indeed, distinct deviations from the scaling law can be seen at some T/H range. In addition, the scaling assumes that the magnetic excitations are localized, but it is open whether the specific heat contains the itinerant magnetic excitations. Moreover, the measurements were performed on powdered sample [34], where the magnetic anisotropy of the specific heat is smeared out.

Thus, examining the relation of the specific heat is an important tool to understand the intrinsic thermodynamic properties of the kagome layers. While specific heat contains both localized and itinerant excitations, thermal conductivity only detects the itinerant contribution. Therefore the combined results of specific heat and thermal conductivity provide pivotal information on the low-energy excitations. In this work, we measured the specific heat C and thermal conductivity κ with high accuracy on single crystals of herbertsmithite. The most important finding is that the intrinsic magnetic contribution of the specific heat in the kagome layers exhibits excellent scaling collapse for T/H. This implies that the specific heat in the kagome layers is governed by localized orphan spins that form random singlets.

II. EXPERIMENTAL

High-quality single crystals were prepared by recrystallization in a three-zone furnace after the prereaction [21]. For the accurate measurements of the specific heat, we used the long relaxation method [46] on a single crystal ($1.5 \times 1.2 \times 0.5$: mm^3, 5.9 mg). The in-plane thermal conductivity was measured on a single crystal with dimensions $1.5 \times 0.7 \times 0.2$: mm^3, which was cut from the crystal used for the specific heat measurements. The thermal conductivity was measured by a standard steady-state method with a one-heater-two-thermometer configuration in dilution refrigerator. The thermal current was applied within the 2D plane. For both measurements, the magnetic field was applied perpendicular to the 2D plane ($\boldsymbol{H} \parallel c$).

III. RESULTS AND DISCUSSION

Figure 2(a) shows the temperature dependence of C is measured up to 15 K in zero and finite magnetic fields.

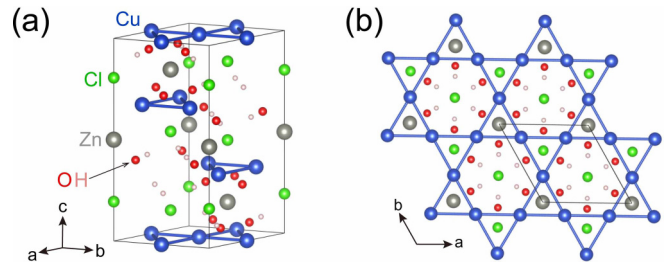

FIG. 1. (a) The unit cell of herbertsmithite $ZnCu_3(OH)_6Cl_2$. ABC-stacked kagome layers composed of Cu are separated by Cl, Zn, and OH. Zn forms an octahedron with oxygens. (b) The top view of a kagome layer. Spins on Cu sites are coupled through Cu-O-Cu superexchange interaction.

Figure 2(b) depicts the T dependence of C in zero and low fields in the low-temperature regime. In zero field, as the temperature is increased, C first increases steeply, showing a shoulder structure, and then increases upwardly. In magnetic fields, the shoulder structure is pronounced, resulting in the broad maximum around 1.5 K. At higher fields above

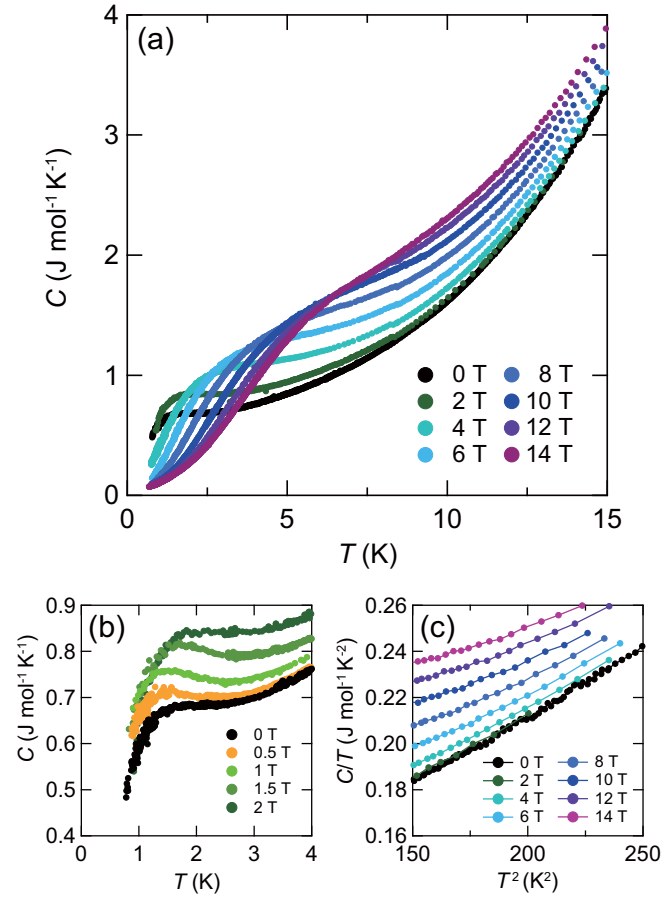

FIG. 2. (a) Temperature dependence of the specific heat in zero and applied magnetic field up to 14 T ($\boldsymbol{H} \parallel c$). (b) C vs T in the low temperature regime at low fields. (c) Specific heat divided by temperature C/T vs T^2 in magnetic field ($\boldsymbol{H} \parallel c$) in the high-temperature regime. To determine the phonon contribution reliably, we measured the specific heat up to above 15 K.

4 T, as shown in Fig. 2(a), C increases monotonically with elevating temperature, showing a hump structure. The hump temperature increases with increasing field. For all fields, C increases upwardly in the high-temperature regime above ∼10 K. As demonstrated in Ref. [45], the raw data in the present study also holds a scaling relation [47]. In addition to the phonon contribution at high temperatures, we found an additional contribution that deviates the specific heat from the scaling function at a low-field region. The detailed analyses discussed below revealed that the contribution is reasonably consistent with the Schottky specific heat arising from the antisite disorder. The deviation is more pronounced below 0.5 T, where previous studies did not measure the specific heat. We measured the low-field region in detail and performed detailed analyses to evaluate the scaling relation of the magnetic specific heat in the following process. (i) We evaluated the phonon and Schottky contribution, (ii) extracted the magnetic contribution by subtracting the phonon and Schottky contributions from the raw data, (iii) showed the scaling plot of the magnetic contribution and quantitatively compared it with the model function.

First we discuss the phonon contribution. As shown in Fig. 2(c), C/T increases in proportion to T^2 at high temperatures for all fields, and the field-dependent data overlap with each other after vertically shifting. This cubic temperature dependence of C is attributed to the acoustic phonon contribution; $C_{\rm ph} = \beta_{\rm ph}T^3$, where $\beta_{\rm ph}$ is the Debye coefficient. From the fitting, we obtain $\beta_{\rm ph} = 6$–7×10^{-4} J mol^{-1} K^{-4}, which corresponds to the Debye temperature of 375–395 K.

As depicted in Fig. 3(a), κ/T in zero field increases almost linearly with temperature, but if we extrapolate κ/T to zero temperature, simply assuming T-linear dependence, κ/T has a negative intercept. In the inset of Fig. 3(a), κ/T is plotted as a function of T^2. Obviously, κ/T increases with decreasing slope. The results of Fig. 3(a) and its inset, which plots κ/T vs T^2, indicate that κ/T depends on T as $\kappa/T \propto T^{\alpha}$ with $1 < \alpha < 2$. The best fit is obtained by $\alpha = 1.3$, as shown by the dotted line in the inset of Fig. 3(a). The power-law temperature dependence is also demonstrated in Fig. 3(b). These results indicate that the residual linear term of the thermal conductivity, $\kappa/T(T \to 0)$, is vanishingly small, if present at all. This provides evidence for the absence of gapless itinerant excitations. We note that the presence or absence of finite $\kappa/T(T \to 0)$ appears to be extremely sensitive to the impurity and disorder levels. In fact, finite $\kappa/T(T \to 0)$ has been reported in $1T - TaS_2$ [48], $EtMe_3Sb[Pd(dmit)_2]_2$ [49,50], $\kappa - H_3$(Cat-EDT-TTF)$_2$ [51], $YbMgGaO_4$ [52], and $Na_2BaCo(PO_4)_2$ [53]. On the other hand, the absence of $\kappa/T(T \to 0)$ has also been suggested in some of these systems [54–57].

The red open circles in Fig. 3(a) and its inset show κ/T in magnetic field of $\mu_0 H = 14$ T. In stark contrast to large field-dependent specific heat shown in Fig. 2(a), the magnetic field has no influence on the thermal conductivity. This field-independent κ indicates that thermal conduction is dominated by phonon contribution, $\kappa \approx \kappa_{\rm ph}$. Moreover, as the magnetic field suppresses the spin-phonon scattering by polarizing spins, the phonon mean-free path increases with magnetic field. The present results, therefore, indicate

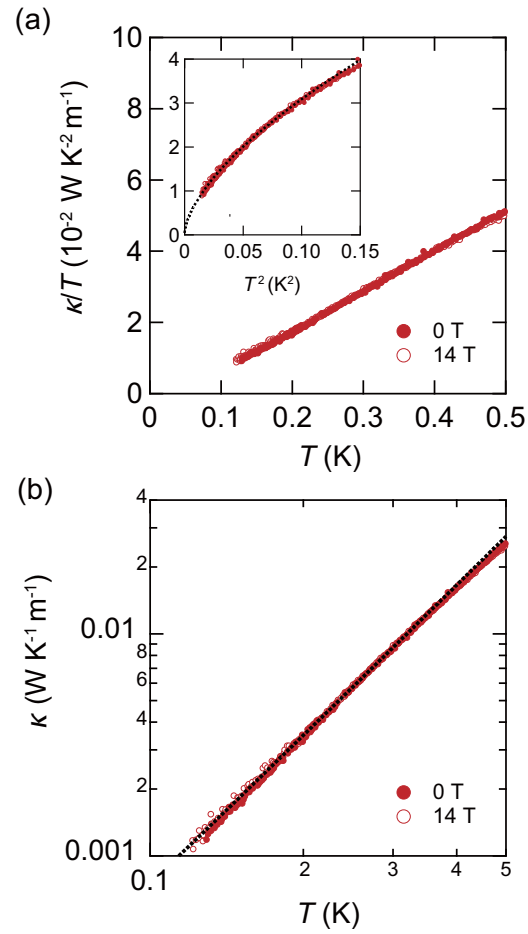

FIG. 3. (a) Thermal conductivity divided by temperature, κ/T, plotted as a function of T. Red filled and open circles represent the data in zero field and applied field of $\mu_0 H = 14$ T ($\boldsymbol{H} \parallel c$), respectively. The inset shows κ/T vs T^2. The dashed line represents $\kappa/T \propto T^{1.3}$. (b) A log-log plot of κ vs T. The dashed line is $\kappa \propto T^{2.3}$.

negligibly small spin-phonon coupling. On the other hand, the broadening of optical phonon mode caused by magnetic excitations indicates non-negligible spin-phonon coupling for optical phonons [58]. This discrepancy is explained by considering the thermal conductivity to be dominated by acoustic phonons at low temperatures.

At low temperatures, $\kappa_{\rm ph}$ is given by $\kappa_{\rm ph} = \frac{1}{3}\beta_{\rm ph}\langle v_s\rangle \ell_{\rm ph} T^3$, where $\langle v_s\rangle$ is the acoustic phonon velocity, and $\ell_{\rm ph}$ is the effective mean-free path of acoustic phonons. When $\ell_{\rm ph}$ becomes comparable to the crystal size at very low temperatures (boundary limit), $\ell_{\rm ph}$ is approximately limited by the effective diameter of the crystal $d_{eff} = 2\sqrt{wt/\pi}$, where w and t are the width and thickness of the crystal, respectively. Using $\beta_{\rm ph} = 6.78 \times 10^{-4}$ J mol^{-1} K^{-4}, $\langle v_s\rangle \approx 3500$ m s^{-1} is obtained. From $w = 0.68$ mm and $t = 0.20$ mm, we estimate the phonon thermal conductivity in the boundary limit $\kappa^b_{\rm ph}/T \approx 2.8 \times 10^{-2}$ W K^{-2} m^{-1} at 0.1 K, which is nearly four times larger than the observed κ/T at the lowest temperature. Thus, $\kappa_{\rm ph}$ is not in the boundary limit even at the lowest temperatures.

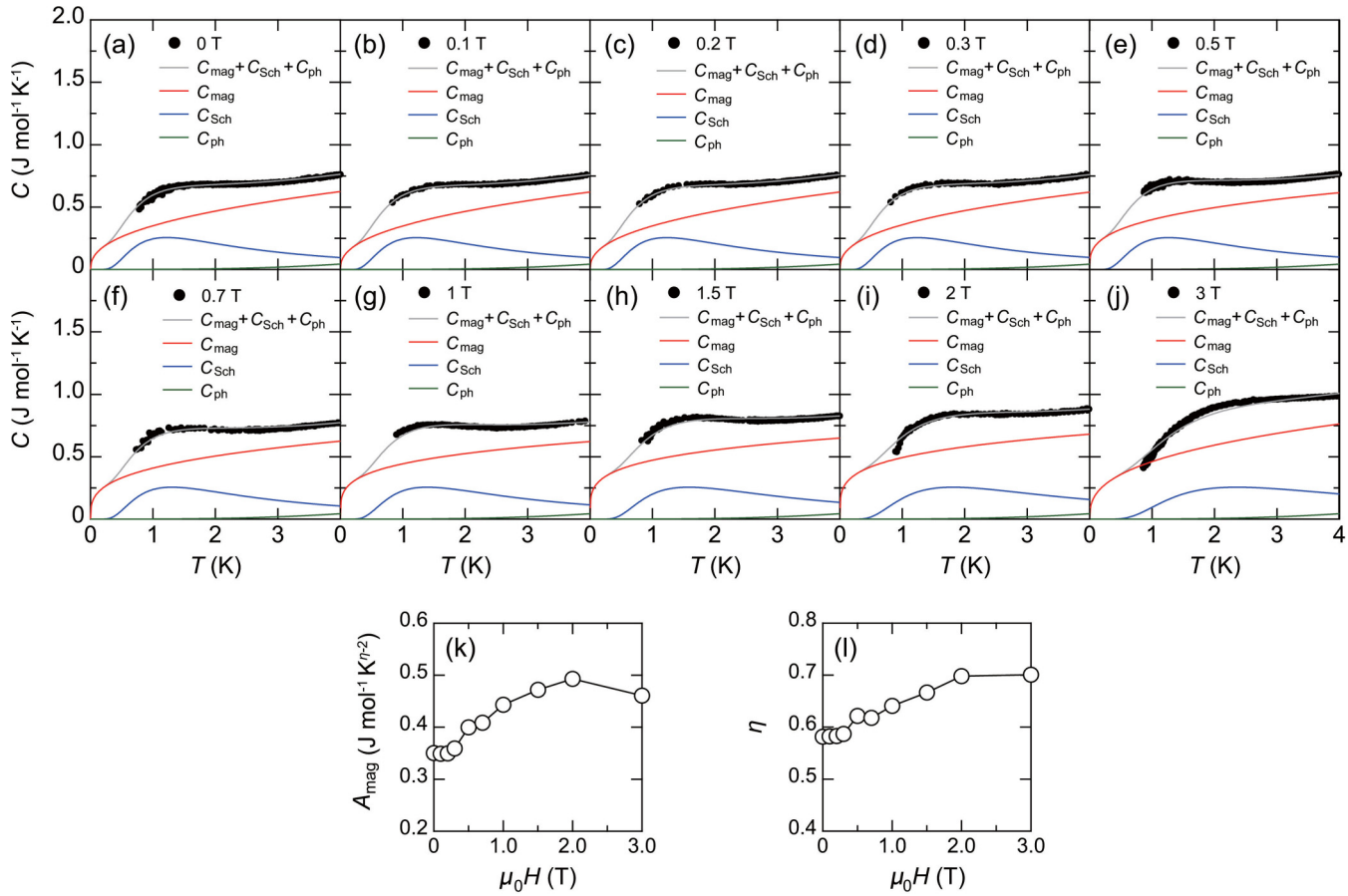

FIG. 4. $C(T)$ vs T in (a) zero and (b)–(j) in small magnetic fields below 4 K, where phonon contribution is negligibly small. $C(T)$ is fitted by the sum of $C_{\rm Sch}$ [Eq. (1)], $C_{\rm ph}$, and $C_{\rm mag}$, assuming power-law temperature dependence of $C_{\rm mag} = A_{\rm mag}T^{1-\eta}$, where $A_{\rm mag}$ and η are constants. Gray lines indicate the results of the fitting. (k) and (l) depict the field dependence of $A_{\rm mag}$ and η obtained by the fitting, respectively.

Having established the absence of itinerant gapless quasiparticle excitations, we analyze the temperature dependence of the specific heat in more detail. We point out that the observed shoulder structure in zero field and broad maximum at weak field of C can be attributed to the two-level Schottky specific heat as

$$C_{\rm Sch} = A_{\rm Sch}\left[\frac{\Delta(H)}{k_B T}\right]^2 \exp\left[-\frac{\Delta(H)}{k_B T}\right], \qquad (1)$$

where $A_{\rm Sch}$ is a constant that is determined by the number of two-level systems. $\Delta(0) = g\mu_B\mu_0 H_0$ is the energy of the excited level, where H_0 is the magnetic field characterized by the crystal electric field and g is the electron g factor assumed to be 2. We assume that the specific heat contains magnetic contribution $C_{\rm mag}$ and is given by $C = C_{\rm ph} + C_{\rm Sch} + C_{\rm mag}$. Figure 4(a) depicts C in zero field below 4 K, where phonon contribution is negligibly small. We try to fit $C(T)$ at low temperatures by assuming power-law temperature dependence of $C_{\rm mag} = A_{\rm mag}T^{1-\eta}$, where $A_{\rm mag}$ and η are constants. As shown in Fig. 4(a), $C(T)$ is well fitted by $A_{\rm Sch} = 0.472(6)$ J mol^{-1} K^{-1}, $\mu_0 H_0 = 1.814(8)$ T, $A_{\rm mag} = 0.350(3)$ J mol^{-1} K$^{\eta-2}$, and $\eta = 0.581(4)$. Surprisingly, as shown in Fig. 5(a), $C(T)$ in zero field is excellently fitted by these three contributions up to 15 K. In the fitting, we used $\beta_{\rm ph} = 6.78 \times 10^{-4}$ J mol^{-1} K^{-4}. We note that the two-level Schottky specific heat likely arises from the interlayer Cu/Zn antisite disorder. The number of two-level obtained from $A_{\rm Sch}$ indicates that nearly 5% of Zn site is replaced by Cu. This value is nearly 1/3 of that reported by NMR [31] and resonant x-ray diffraction [22] measurements. The reason for this discrepancy between the measurements is not clear. To confirm the validity of the present analysis, we fit the low-temperature data at low fields, where $C(T)$ exhibits a broad maximum shown in Fig. 2(b). In the fitting, we fixed $C_{\rm ph}$ and calculated $C_{\rm Sch}$ with the Schottky gap in magnetic fields,

$$\Delta(H) = g\mu_B\mu_0\sqrt{H^2 + H_0^2}. \qquad (2)$$

Here we used $A_{\rm Sch}$ and H_0 obtained from the fitting of zero-field data. As shown in Figs. 4(b)–4(l), $C(T)$ is well fitted in this temperature range by assuming the power-law-dependent $C_{\rm mag}$. The field dependence of $A_{\rm mag}$ and η are shown in Figs. 4(k) and 4(l), respectively. In contrast to the excellent fitting in zero-field $C(T)$ in the whole temperature regime, $C(T)$ starts to deviate at high temperatures when magnetic fields are applied. In what follows, to extract $C_{\rm mag}$, we use $C_{\rm Sch}$ calculated from Eq. (1) with $\Delta(H)$ given by Eq. (2). Moreover, $C_{\rm ph}$ is calculated by assuming field-independent $\beta_{\rm ph} = 6.78 \times 10^{-4}$ J mol^{-1} K^{-4}, which is justified by the field-independent thermal conductivity.

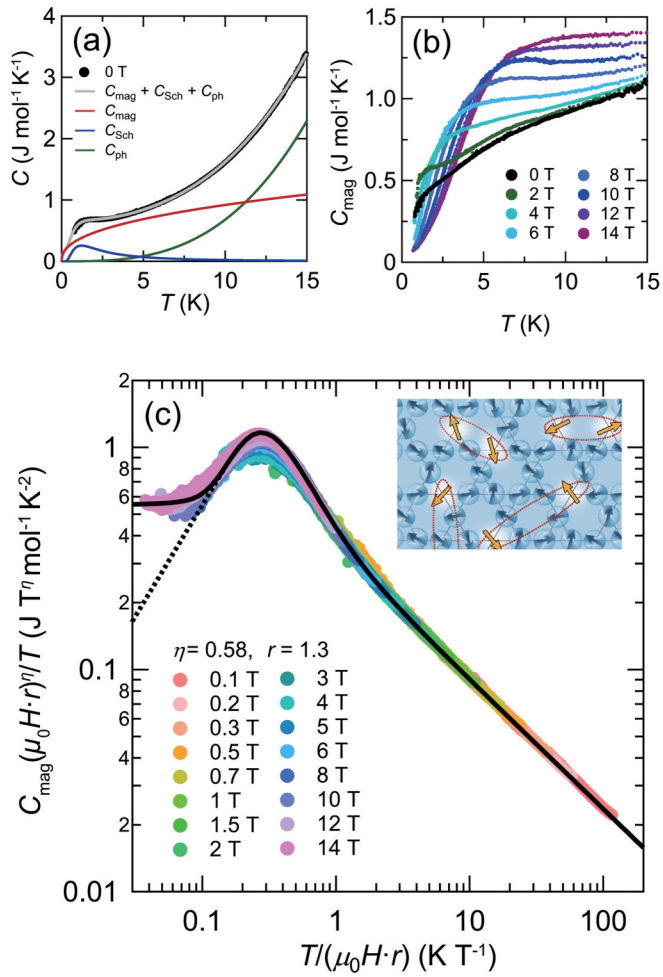

FIG. 5. (a) Specific heat C in zero field plotted as a function of T. The gray line represents the sum of phonon (green line), Schottky (blue) and magnetic (red) contributions. (b) Temperature dependence of magnetic contribution $C_{\rm mag}$ in zero and applied magnetic fields obtained by subtracting $C_{\rm Sch}$ and $C_{\rm ph}$ from total C. (c) Scaling relationship of magnetic contribution of the specific heat; $C_{\rm mag}(\mu_0 Hr)^{\eta}/T$ plotted as a function of $T/(\mu_0 Hr)$. Excellent scaling is observed with $r = 1.3$. Solid and dotted black lines, respectively, indicate the scaling function F_0 and F_1 in Eq. (3) with coefficients $\eta = 0.58, A_{\rm mag} = 0.35$.

Figure 5(b) depicts the T dependence of $C_{\rm mag}$ obtained by subtracting $C_{\rm ph}$ and $C_{\rm Sch}$. Recently, new theoretical studies of the role of quenched disorder in quantum paramagnetic states including QSL have been proposed [44,45]. In this picture, as shown schematically in the inset of Fig. 5(c), the majority of spin-1/2 sites form a quantum paramagnetic state such as a spin liquid, while a small fraction of sites host nucleated orphan spins, which need not be microscopic defects but rather could be emergent quantum objects that can arise from a competition of disorder and frustration. An orphan spin can couple with another orphan spin to form a singlet state. The exchange energies between these orphan spins vary randomly, with an exponential dependence on their distance, which leads to a formation of singlets with random energy gaps whose distribution is exponentially broad. This broad distribution includes singlets with arbitrarily small energy gaps. This model predicts that $C_{\rm mag}$ arising from the localized spin excitations collapses into a single curve of form,

$$\frac{C_{\rm mag}(H,T)}{T} \sim \frac{1}{H^{\eta}} F_q(T/H), \tag{3}$$

where $F_q(X)$ is a scaling function, which is determined by the energy distribution of the random singlets;

$$F_q(X) \sim \begin{cases} X^q & X \ll 1 \\ X^{-\eta}(1 + c_0/X^2) & X \gg 1. \end{cases} \tag{4}$$

Here $q = 1$ and $q = 0$ correspond to the case with and without Dzyaloshinskii-Moriya (DM) interactions in the effective (emergent) low-energy theory coupling the orphan spins, respectively. η is a nonuniversal exponent, $0 \leqslant \eta \leqslant 1$, that characterizes the probability distribution of antiferromagnetic exchange energies $P(J) \sim J^{-\eta}$. The spins with exchange $J < k_B T$ behave as free spins and $C(T)$ shows power-law dependence on T as $C \propto T^{1-\eta}$. When $\eta \neq 0$, $F_q(X)$ increases with X, peaks and decreases at large X, saturating for $q = 0$. It should be stressed that the power-law temperature dependence of $C(T)$ in zero field is also consistently given by this scaling and determines η uniquely.

In Fig. 5(c), $C_{\rm mag}(\mu_0 Hr)^{\eta}/T$ is plotted as a function of $T/(\mu_0 Hr)$. Here $r = g_o/2$, where g_o is the effective g factor of orphan spin, which can differ from $g = 2$ or from the single-site g factor due to renormalization group (RG) flow of spin orbit coupling in the emergence of non-on-site orphan spins. We find that $C_{\rm mag}$ at all fields collapse into a single curve. Letting the g factor be a fitting parameter, we find the best fit was obtained by $r = 1.3$, equivalently $g_o = 2.6$. We note that the data is reasonably fitted by using $g_o = 2.1$–2.3 reported by electron paramagnetic resonance measurements [59]. Moreover, $C_{\rm mag}$ holds a scaling relation even if we assume $r = 1$ as in Refs. [45,60]. However, without tuning r, while the scaling relation is satisfied, the experimental data quantitatively deviates from the scaling function $F(T/H)$, which is proposed in Ref. [45]. After determining the scaling coefficients, r and η, one by one, we evaluated the fitting with the model function and found that those coefficients were fully optimized [47].

The scaling function obtained by the fit to F_0 in Eq. (3) is shown by the solid black line. Thus $C_{\rm mag}$ exhibits an excellent scaling collapse with a universal scaling function. At $T/(\mu_0 Hr) < 0.1$, $C_{\rm mag}(\mu_0 Hr)^{\eta}/T$ becomes constant, suggesting $q = 0$. To confirm this, it is necessary to measure the specific heat precisely at $T/(\mu_0 Hr) \ll 0.1$, where the specific heat is dominated by the nuclear Schottky anomaly, which makes it difficult to evaluate the magnetic excitations [45].

The scaling law provides several pieces of important information on the QSL state in herbertsmithite. The result suggests that the specific heat contains substantial contributions from the frustrated kagome layers. In addition, the quantum fluctuations in kagome layers sensitively respond to randomness. In herbertsmithite, randomness is likely

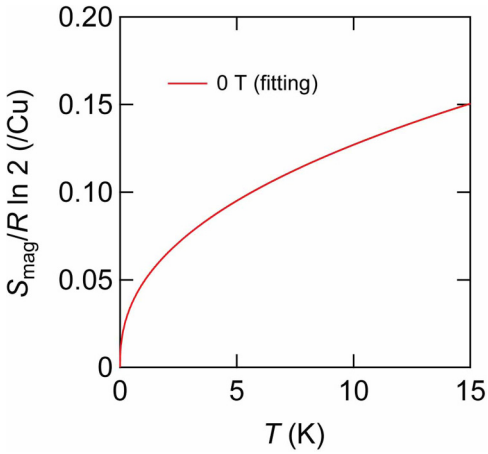

FIG. 6. The entropy per Cu site normalized by $R\ln 2$ is calculated by the formula $S_{\rm mag}/R\ln 2 = (1/R\ln 2)\times\int_0^T \frac{C'_{\rm mag}(T')}{T'}dT'$. $C'_{\rm mag} = A_{\rm mag}T^{1-\eta}$ ($A_{\rm mag} = 0.35$, $\eta = 0.58$) is the fitting function of $C_{\rm mag}$ at 0 T.

attributable to the exchange bond disorder in the perfect kagome lattice, which is caused by the interlayer Cu/Zn antisite disorder. In fact, the Jahn-Teller effect causes a local structural distortion around the Cu defects in the Zn planes [61], which gives rise to the exchange bond disorder of Cu ions in the kagome layer just above and below the defects. If antisite disorder with Cu spins on interlayer sites are reasonably decoupled from the kagome layers, their density can be estimated from their Schottky anomaly contribution to specific heat, giving 5% of Zn sites (equivalently a density of 1.7% of overall Cu sites). However, the entropy associated with the scaling part of $C(T)$, estimated by $S_{\rm mag}/R\ln 2 = (1/R\ln 2)\times\int_0^T \frac{C'_{\rm mag}(T')}{T'}dT'$, reaches much larger value of 0.05 (per Cu site) already by $T = 1$ K, rising to 0.1 by $T = 5$ K (Fig. 6). It therefore seems inconsistent to attribute the specific heat scaling purely to Zn/Cu defect spins (or, at the very least, such spins cannot be considered as independent variables).

Let us now discuss the relationship between the current results to previous studies relating herbertsmithite to random singlet type physics. References [34,45] found scaling of the specific heat as in Eq. (4), but with $q = 1$, rather than $q = 0$. As discussed in Ref. [45], q is determined by the presence or absence of DM coupling in the low-energy effective theory, which is not the same as the microscopic lattice scale theory for herbertsmithite. In particular, microscopically allowed DM coupling may or may not survive the RG flow to the effective low-energy interactions, leading to either $q = 1$ or $q = 0$, depending on the environment of the coupled orphan spins. We thus speculate that the nature of the orphan spins may be somewhat different here as opposed to in Refs. [34,45], which could lead to the differing $q = 0, 1$ values. Heavy fermion and related random singlet type physics are also discussed in Ref. [41], which reports multiple scaling behavior in ac susceptibility, with magnetic fields and dynamical frequency, and in the dynamical structure factor from inelastic neutron scattering. Interestingly, Ref. [41] points out that a distribution of impurity couplings extending up to several meV is necessary to model the observations, which would be surprisingly large for out-of-plane impurity ions; however, in the present picture that also involves orphan spins in the kagome planes, such a distribution may be more natural. Finally, Ref. [30] considers out-of-plane impurity spins, modeled as a diluted simple cubic lattice, and uses this model to capture previously measured specific heat as a function of temperature below 1.25 K at zero magnetic field [34]. This zero-field model gives an estimate of Schottky contribution that differs from the present analysis.

A spin liquid phase could also contribute to the specific heat. $C_{\rm mag}$ contains both the orphan spin and the spin liquid contributions. The reported spin gap Δ_s at zero field is comparable to the applied field in this study; $\Delta_s/J \sim 0.03$–0.07 by the NMR study [31] and $\Delta_s \sim 0.7$ meV by the neutron study [30]. The recent NMR study reports the broad distribution of spin gap energy [33]. If the spin gap closes by the field, $C_{\rm mag}$ at high fields can contain the spin liquid contribution, in addition to the orphan spin contribution. Even if this is the case, our results indicate that the contribution of the spin liquid is not significant even at 14 T; or, if any spin liquid gap closing occurs, it may occur in such a way that its contribution is similar to the contribution from a random singlet regime. For example, the gap closing might occur in a random inhomogeneous pattern with similar scaling as random singlets (this is not unreasonable for a spin liquid made out of fluctuating singlet pairs). However, given that the field dependence of the spin gap depends on the particular type of spin liquid, it is an open question whether our scaling result is compatible with observations of the small spin gap [30,31,33].

We point out that the orphan spins in the kagome layers also largely contribute to the magnetic susceptibility, which exhibits a diverging behavior with decreasing temperature, although the quantitative analysis is difficult compared with the specific heat. Rather, the ground state of this system is the QSL state originated from the quantum fluctuations and frustration. Randomness induces a fraction of orphan spins forming localized random singlets in the kagome layers. Finally, we note that a similar scaling relation of the specific heat has been reported in 1T-TaS_2, a triangular lattice system, which may form spinon Fermi surface [48]. Given that the present results of herbertsmithite provide strong support for similar $q = 0$ scaling collapse in Ref. [45], taken together these results hint at a potentially universal feature for QSLs with weak randomness.

In summary, we measured the specific heat and thermal conductivity on single crystals of herbertsmithite. Thermal conductivity reveals the absence of gapless itinerant excitations. Our result is highlighted by an excellent scaling collapse for T/H of the intrinsic magnetic contribution of the specific heat in the kagome layers. These results demonstrate that the specific heat in the kagome layers is governed by localized orphan spins that form random singlets, which are surrounded by the quantum spin liquid. The present study provides vital information on how the quantum fluctuations respond to randomness due to quenched disorder, which is key for fundamental understanding the mysterious QSL states.

Note added. Recently, we became aware of Ref. [60]. Our thermal conductivity result, the absence of itinerant quasiparticle excitations, is consistent with Ref. [60]. However, the

conclusions regarding the validity of the scaling relation of the specific heat are different; this may be due to a difference in the way specific heat is analyzed. In the present case, by subtracting the phonon and Schottky contributions, we extracted the magnetic contribution, which is a key ingredient to examine the scaling theory.

ACKNOWLEDGMENTS

We thank H. Kawamura, Z. Hiroi, and K. Totsuka for helpful discussions. This work was supported by JSPS KAKENHI Grants No. JP19J21017, No. JP18H05227 and JST CREST (No. JP-MJCR19T5).

[1] S. Sachdev, Phys. Rev. B **45**, 12377 (1992).
[2] Y. Ran, M. Hermele, P. A. Lee, and X.-G. Wen, Phys. Rev. Lett. **98**, 117205 (2007).
[3] R. R. P. Singh and D. A. Huse, Phys. Rev. B **76**, 180407(R) (2007).
[4] M. Hermele, Y. Ran, P. A. Lee, and X.-G. Wen, Phys. Rev. B **77**, 224413 (2008).
[5] H. C. Jiang, Z. Y. Weng, and D. N. Sheng, Phys. Rev. Lett. **101**, 117203 (2008).
[6] Y. Ran, W.-H. Ko, P. A. Lee, and X.-G. Wen, Phys. Rev. Lett. **102**, 047205 (2009).
[7] O. Götze, D. J. J. Farnell, R. F. Bishop, P. H. Y. Li, and J. Richter, Phys. Rev. B **84**, 224428 (2011).
[8] S. Yan, D. A. Huse, and S. R. White, Science **332**, 1173 (2011).
[9] H.-C. Jiang, Z. Wang, and L. Balents, Nature Phys. **8**, 902 (2012).
[10] S. Depenbrock, I. P. McCulloch, and U. Schollwöck, Phys. Rev. Lett. **109**, 067201 (2012).
[11] S. Nishimoto, N. Shibata, and C. Hotta, Nature Commun. **4**, 2287 (2013).
[12] Y. Iqbal, F. Becca, S. Sorella, and D. Poilblanc, Phys. Rev. B **87**, 060405(R) (2013).
[13] B. K. Clark, J. M. Kinder, E. Neuscamman, Garnet Kin-Lic Chan, and M. J. Lawler, Phys. Rev. Lett. **111**, 187205 (2013).
[14] H. Kawamura, K. Watanabe, and T. Shimokawa, J. Phys. Soc. Jpn. **83**, 103704 (2014).
[15] Y.-C. He, M. P. Zaletel, M. Oshikawa, and F. Pollmann, Phys. Rev. X **7**, 031020 (2017).
[16] A. M. Läuchli, J. Sudan, and R. Moessner, Phys. Rev. B **100**, 155142 (2019).
[17] H. Kawamura and K. Uematsu, J. Phys.: Condens. Matter **31**, 504003 (2019).
[18] P. Mendels and F. Bert, J. Phys. Soc. Jpn. **79**, 011001 (2010).
[19] M. R. Norman, Rev. Mod. Phys. **88**, 041002 (2016).
[20] M. P. Shores, E. A. Nytko, B. M. Bartlett, and D. G. Nocera, J. Am. Chem. Soc. **127**, 13462 (2005).
[21] T. H. Han, J. S. Helton, S. Chu, A. Prodi, D. K. Singh, C. Mazzoli, P. Müller, D. G. Nocera, and Y. S. Lee, Phys. Rev. B **83**, 100402(R) (2011).
[22] D. E. Freedman, T. H. Han, A. Prodi, P. Müller, Q.-Z. Huang, Y.-S. Chen, S. M. Webb, Y. S. Lee, T. M. McQueen, and D. G. Nocera, J. Am. Chem. Soc. **132**, 16185 (2010).
[23] O. Ofer, A. Keren, E. A. Nytko, M. P. Shores, B. M. Bartlett, D. G. Nocera, C. Baines, and A. Amato, arXiv:cond-mat/0610540.
[24] P. Mendels, F. Bert, M. A. de Vries, A. Olariu, A. Harrison, F. Duc, J. C. Trombe, J. S. Lord, A. Amato, and C. Baines, Phys. Rev. Lett. **98**, 077204 (2007).
[25] F. Bert, S. Nakamae, F. Ladieu, D. L'Hôte, P. Bonville, F. Duc, J.-C. Trombe, and P. Mendels, Phys. Rev. B **76**, 132411 (2007).
[26] T. H. Han, J. S. Helton, S. Chu, D. G. Nocera, J. A. Rodriguez-Rivera, C. Broholm, and Y. S. Lee, Nature (London) **492**, 406 (2012).
[27] A. Olariu, P. Mendels, F. Bert, F. Duc, J. C. Trombe, M. A. de Vries, and A. Harrison, Phys. Rev. Lett. **100**, 087202 (2008).
[28] T. Imai, E. A. Nytko, B. M. Bartlett, M. P. Shores, and D. G. Nocera, Phys. Rev. Lett. **100**, 077203 (2008).
[29] G. J. Nilsen, M. A. de Vries, J. R. Stewart, A. Harrison, and H. M. Rønnow, J. Phys.: Condens. Matter **25**, 106001 (2013).
[30] T. H. Han, M. R. Norman, J. J. Wen, J. A. Rodriguez-Rivera, J. S. Helton, C. Broholm, and Y. S. Lee, Phys. Rev. B **94**, 060409(R) (2016).
[31] M. Fu, T. Imai, T.-H. Han, and Y. S. Lee, Science **350**, 655 (2015).
[32] P. Khuntia, M. Velazquez, Q. Barthélemy, F. Bert, E. Kermarrec, A. Legros, B. Bernu, L. Messio, A. Zorko, and P. Mendels, Nature Phys. **16**, 469 (2020).
[33] J. Wang, W. Yuan, P. M. Singer, R. W. Smaha, W. He, J. Wen, Y. S. Lee, and T. Imai, Nature Phys. **17**, 1109 (2021).
[34] J. S. Helton, K. Matan, M. P. Shores, E. A. Nytko, B. M. Bartlett, Y. Yoshida, Y. Takano, A. Suslov, Y. Qiu, J. H. Chung, D. G. Nocera, and Y. S. Lee, Phys. Rev. Lett. **98**, 107204 (2007).
[35] M. A. de Vries, K. V. Kamenev, W. A. Kockelmann, J. Sanchez-Benitez, and A. Harrison, Phys. Rev. Lett. **100**, 157205 (2008).
[36] T. Han, S. Chu, and Y. S. Lee, Phys. Rev. Lett. **108**, 157202 (2012).
[37] V. R. Shaginyan, A. Z. Msezane, K. G. Popov, G. S. Japaridze, and V. A. Stephanovich, Europhys. Lett. **97**, 56001 (2012).
[38] T.-H. Han, R. Chisnell, C. J. Bonnoit, D. E. Freedman, V. S. Zapf, N. Harrison, D. G. Nocera, Y. Takano, and Y. S. Lee, arXiv:1402.2693.
[39] J. Schnack, J. Schulenburg, and J. Richter, Phys. Rev. B **98**, 094423 (2018).
[40] M. Rigol and R. R. P. Singh, Phys. Rev. Lett. **98**, 207204 (2007).
[41] J. S. Helton, K. Matan, M. P. Shores, E. A. Nytko, B. M. Bartlett, Y. Qiu, D. G. Nocera, and Y. S. Lee, Phys. Rev. Lett. **104**, 147201 (2010).
[42] B. Bernu and C. Lhuillier, Phys. Rev. Lett. **114**, 057201 (2015).
[43] C. Hotta and K. Asano, Phys. Rev. B **98**, 140405(R) (2018).
[44] I. Kimchi, A. Nahum, and T. Senthil, Phys. Rev. X **8**, 031028 (2018).
[45] I. Kimchi, J. P. Sheckelton, T. M. McQueen, and P. A. Lee, Nature Commun. **9**, 4367 (2018).
[46] O. J. Taylor, A. Carrington, and J. A. Schlueter, Phys. Rev. Lett. **99**, 057001 (2007).

[47] See Supplemental Material at http://link.aps.org/supplemental/10.1103/PhysRevB.106.174406 for the evaluation of the scaling coefficients and the scaling plot for the raw data.
[48] H. Murayama, Y. Sato, T. Taniguchi, R. Kurihara, X. Z. Xing, W. Huang, S. Kasahara, Y. Kasahara, I. Kimchi, M. Yoshida, Y. Iwasa, Y. Mizukami, T. Shibauchi, M. Konczykowski, and Y. Matsuda, Phys. Rev. Res. **2**, 013099 (2020).
[49] M. Yamashita, N. Nakata, Y. Senshu, M. Nagata, H. M. Yamamoto, R. Kato, T. Shibauchi, and Y. Matsuda, Science **328**, 1246 (2010).
[50] M. Yamashita, Y. Sato, T. Tominaga, Y. Kasahara, S. Kasahara, H. Cui, R. Kato, T. Shibauchi, and Y. Matsuda, Phys. Rev. B **101**, 140407(R) (2020).
[51] M. Shimozawa, K. Hashimoto, A. Ueda, Y. Suzuki, K. Sugii, S. Yamada, Y. Imai, R. Kobayashi, K. Itoh, S. Iguchi, M. Naka, S. Ishihara, H. Mori, T. Sasaki, and M. Yamashita, Nature Commun. **8**, 1821 (2017).
[52] X. Rao, G. Hussain, Q. Huang, W. J. Chu, N. Li, X. Zhao, Z. Dun, E. S. Choi, T. Asaba, L. Chen, L. Li, X. Y. Yue, N. N. Wang, J.-G. Cheng, Y. H. Gao, Y. Shen, J. Zhao, G. Chen, H. D. Zhou, and X. F. Sun, Nature Commun. **12**, 4949 (2021).
[53] N. Li, Q. Huang, X. Y. Yue, W. J. Chu, Q. Chen, E. S. Choi, X. Zhao, H. D. Zhou, and X. F. Sun, Nature Commun. **11**, 4216 (2020).
[54] Y. Xu, J. Zhang, Y. S. Li, Y. J. Yu, X. C. Hong, Q. M. Zhang, and S. Y. Li, Phys. Rev. Lett. **117**, 267202 (2016).
[55] Y. J. Yu, Y. Xu, L. P. He, M. Kratochvilova, Y. Y. Huang, J. M. Ni, L. Wang, S.-W. Cheong, J.-G. Park, and S. Y. Li, Phys. Rev. B **96**, 081111(R) (2017).
[56] P. Bourgeois-Hope, F. Laliberté, E. Lefrançois, G. Grissonnanche, S. R. de Cotret, R. Gordon, S. Kitou, H. Sawa, H. Cui, R. Kato, L. Taillefer, and N. Doiron-Leyraud, Phys. Rev. X **9**, 041051 (2019).
[57] J. M. Ni, B. L. Pan, B. Q. Song, Y. Y. Huang, J. Y. Zeng, Y. J. Yu, E. J. Cheng, L. S. Wang, D. Z. Dai, R. Kato, and S. Y. Li, Phys. Rev. Lett. **123**, 247204 (2019).
[58] A. B. Sushkov, G. S. Jenkins, T.-H. Han, Y. S. Lee, and H. D. Drew, J. Phys.: Condens. Matter **29**, 095802 (2017).
[59] A. Zorko, M. Herak, M. Gomilšek, J. van Tol, M. Velázquez, P. Khuntia, F. Bert, and P. Mendels, Phys. Rev. Lett. **118**, 017202 (2017).
[60] Y. Y. Huang, Y. Xu, L. Wang, C. C. Zhao, C. P. Tu, J. M. Ni, L. S. Wang, B. L. Pan, Y. Fu, Z. Hao, C. Liu, J.-W. Mei, and S. Y. Li, Phys. Rev. Lett. **127**, 267202 (2021).
[61] S.-H. Lee, H. Kikuchi, Y. Qiu, B. Lake, Q. Huang, K. Habicht, and K. Kiefer, Nature Mater. **6**, 853 (2007).

Correction: An affiliation indicator ascribed to the first author has been removed and the associated institution now appears in a byline footnote as a present address.